

Petrographic and petrophysical characterization of the main aerial and hydraulic mortars used in the construction and rehabilitation sectors

 C. Parra-Fernández^a ,  M.J. Varas-Muriel^{b,c}

a. Departamento de Mineralogía y Petrología, Universidad de Granada, (Granada, Spain)
b. Departamento de Mineralogía y Petrología, Universidad Complutense de Madrid, (Madrid, Spain)
c. Instituto de Geociencias (CSIC-UCM), (Madrid, Spain)

 : clarapf@ugr.es

Received March 15, 2024

Accepted July 29, 2024

Available on line March 25, 2025

ABSTRACT: Petrographic and petrophysical characterization of aerial and hydraulic mortars allows their differentiation and the establishment of their most suitable applications. Natural, aerial or hydraulic lime mortars as well as artificial cements mortars present different physical properties. It shall be noted that physical characteristics, which depend on petrographic characteristics, impact on its mechanical properties. Therefore, this comparative study with standardised techniques and tests, has analysed these mortars from a petrographic, petrophysical and mechanical point of view. The chemical processes and porosity originated during mortar production and subsequent curing phase explain mortar physical behaviour (hardness, strength, as well as fluid access and retention). This study confirms that air lime mortars are the most porous and least resistant while cement mortars are the most resistant and impermeable. Finally, natural hydraulic lime mortars, with petrographic characteristics similar to cement mortars, have physical-mechanical properties close to aerial ones, although they are more impermeable and resistant.

KEY WORDS: Hydraulic mortars; Aerial mortars; Petrographic characterization; Petrophysical properties; Suitable applications.

Citation/Citar como: Parra-Fernández C, Varas-Muriel M. 2025. Petrographic and petrophysical characterization of the main aerial and hydraulic mortars used in the construction and rehabilitation sectors. Mater. Construcc. 75(357):e367. <https://doi.org/10.3989/mc.2025.379124>.

RESUMEN: *Caracterización petrográfica y petrofísica de los principales morteros aéreos e hidráulicos usados en los sectores de la construcción y la rehabilitación*. La caracterización petrográfica y petrofísica de los morteros aéreos e hidráulicos permite distinguirlos y establecer sus aplicaciones más adecuadas. Los morteros de cales naturales, aéreas o hidráulicas, y cementos artificiales, presentan diferentes propiedades físicas. Estas, dependen de sus características petrográficas y repercuten en sus propiedades mecánicas. Por ello, este estudio comparativo con técnicas y ensayos normalizados ha analizado estos morteros desde un punto de vista petrográfico, petrofísico y mecánico. Los procesos químicos y porosidad originados durante la elaboración y posterior curado de los morteros explican su comportamiento físico (dureza, resistencia, acceso y retención de fluidos). Este estudio confirma que los morteros de cal aérea son los más porosos y menos resistentes, mientras que los de cemento son los más resistentes e impermeables. Asimismo, los morteros de cales hidráulicas naturales, con características petrográficas semejantes a los de cemento, presentan propiedades físico-mecánicas similares a los aéreos, aunque son más impermeables y resistentes.

PALABRAS CLAVE: Morteros hidráulicos; Morteros aéreos; Caracterización petrográfica; Propiedades petrofísicas; Usos adecuados.

Copyright: © 2025 CSIC. This is an open-access article distributed under the terms of the Creative Commons Attribution 4.0 International (CC BY 4.0) License.

1. INTRODUCTION

Mortars are building materials made by mixing binders with aggregates and water (1). Since the beginning of the construction activity, the main uses of this type of materials were to join structural elements, to cover surfaces such as floors and walls as well as to act as waterproofing barriers (2).

Conglomerate stones were used even before natural stone due to the lack of outcrops and extraction tools and have been evolving at the same time as the processing techniques of the binders (3, 4). Historically, binders were geological materials such as clays to which water was added to increase their workability (5) or bitumen, used in mortars in Mesopotamian times (6), but nowadays most binders (gypsum, limes and Portland cement) are the result of a pyrotechnological process.

Ancient and modern binders can be grouped according to their setting mechanisms, which is more useful for defining their construction times and applications. Thus, aerial binders, such as aerial lime, are those in which the carbonation process can take years and only occurs in the presence of air when reacting with atmospheric CO₂. On the other hand, hydraulic binders, such as hydraulic lime and cement, harden by partially reacting with water and also with CO₂, taking place to much faster setting times (1 to 6 months or 2-4 days, depending on the degree of hydraulicity of the lime, and few hours in the case of cement (7, 8).

Aerial or hydraulic binders' characteristics are due to the composition and required thermal processing of their raw materials. In this manner, air lime is a binder that can be obtained from calcination at 800-1000 °C of pure limestones (CaCO₃), giving rise to a *fatty lime*, or can also be obtained from dolomites (CaMg(CO₃)₂) giving rise to a *lean lime*. Likewise, hydraulic binders, such as natural hydraulic limes and Portland cements are the product of a series of processes with variable medium-high temperatures (900-1450 °C) and low pressures, which result in chemical reactions and mineral phases (calcium silicates, calcium aluminates and aluminum-calcium silicates), similar to those that occur geologically in contact metamorphism.

Natural hydraulic limes come from the calcination of clayey or siliceous limestones (9) with impurities of silica and alumina at temperatures below 1250 °C (10, 11). In contrast, ordinary Portland cement is produced by calcining limestone and clays (20-25%) at high temperatures (> 1300 °C), which are subsequently mixed with up to 3% of a setting retardant as gypsum (12).

In hydraulic binders, during calcination, the raw material decomposes into calcium, silicon, aluminium and iron oxides and forms hydraulic phases (calcium silicates and/or aluminates, and calcium ferrite-aluminates). These mineral phases, when hydrated, then define the hydraulic character and the ability of the binder to set and harden under water (10). Finally, the manufacturing process, in vertical continuous or discontinuous lime kilns or in horizontal rotary cement kilns and the addition of additives influence the nature of the final products (2, 3, 11, 13, 14).

Traditionally, lime has been the most widely used binder throughout history until the appearance of artificial cement in the early 19th century (1), a time in which the dominance of lime was transferred to cement due to its good mechanical properties and fast setting times. However, in recent decades, it has been noted that when Portland cement has been used for restoration purposes or in soft materials, it has had negative effects by increasing the deterioration process of stone, mortar and other building materials and causing irreversible damage even when it has been removed (15-20). Consequently, the above reasons explain why Portland cement is currently discarded for restoration and rehabilitation purposes and other binders are recommended for these uses.

In ancient and medieval monuments, mortars are an important part of the structures and contribute significantly to their stability (21, 22), so the use of materials that are chemically or mechanically incompatible compromises the construction integrity. Likewise, to restore historic materials without causing incompatibilities or deterioration pathologies, it is important to know their intrinsic properties (hardness, stiffness, impermeability, etc.) (3, 17, 23).

Thus, air lime offers an easy workability, slow hardening, high permeability to water and water vapour and absence of soluble salts (1, 24, 25), which has multiple benefits in the restoration and conservation of ancient buildings. However, due to its slow setting time, high deformation behaviour and low durability against external agents, it is not always compatible with the timescales and mechanical strengths required in the new construction sector.

Likewise, natural hydraulic lime mortars (NHL), are also used in historic building interventions for structural works, to repair damaged mortars, replace harmful binders and to protect historic fabric (4, 26-31). Nevertheless, NHL mortars are also currently used in construction and bioconstruction sectors due to their features as sustainable building materials. These properties can be grouped into manufacturing temperatures much lower than those used to produce other modern binders and the high-water vapour permeability and breathability coefficients of their mortars (4, 17, 32-34).

In the last decades, the characterization of artificial and natural binders in ancient and modern mortars (18th-19th centuries) has increased because of the need to know their state of preservation, environmental resistance, raw materials, manufacturing techniques, etc. (4, 7, 25, 29, 30, 35-39) to reproduce them in new construction and restoration works. Similarly, assessing the compatibility and durability of mortars with other building materials from an aesthetic, chemical-mineralogical and physical-mechanical point of view is nowadays a pursued objective, which also makes it possible to avoid cost overruns and to control inappropriate uses.

Due to the current interest on this topic, there are recent standards (e.g. EN 17187: 2020 (40)) that provide guidance on tests and techniques for the characterization of mortars used in cultural heritage (25, 39) and that can be extrapolated to the study of modern mortars to allow their intercomparison.

Thus, the aim of this work is to establish the basis for the characterization and distinction of different types of mortars by using different analytical techniques and tests that are included in the EN 17187:2020 standard (40). For this purpose, the petrographic and petrophysical properties of four mortars made with different current binders (air lime, natural hydraulic limes, and Portland cement) have been evaluated and compared.

2. MATERIALS AND METHODS

2.1. Materials

The studied materials in this work are an aerial lime, two types of natural hydraulic lime and an ordinary Portland cement. The air lime is a CL90-S PL (hydrated calcium lime in paste) from the company PROIESCON S.L. and the natural hydraulic limes a NHL2 and NHL5 (non-additivated, feebly, and eminently hydraulic binders) from the Saint Astier company. The limestone-additivated Portland cement (CEM II/ B-L 32.5 N) is an artificial hydraulic binder produced by Lafarge-Holcim. All types of limes are regulated by EN 459-1: 2015 standard (9) while cement is regulated by EN 197-1: 2011 (41) and RC-16 (2016) (42).

A total of 36 mortar samples were made with coarse siliceous sand aggregate (1-2 mm). Nine of each type of binder: 3 prismatic samples of 10x10x4 cm, 3 prismatic samples of 16x4x4 cm and 3 square plates of 5x5x1 cm. The binder: aggregate ratio was 2:3 and the curing period of the mortars prior to the start of the tests was 90 days. The curing conditions for all mortars were > 80% RH for the first 7 days and approximately 60% RH at a temperature of 20-25°C until 90 days. The 90-days curing period was selected on the basis of previous studies on both air and hydraulic limes (43-46) and due to it was considered sufficient time for further handling and evaluation of the physical and mechanical behaviour of the limes, especially air lime.

The following abbreviations were used: CL90-S PL (air lime mortar), NHL2 (natural hydraulic lime NHL2 mortar), NHL5 (natural hydraulic lime NHL5 mortar) and OPC (ordinary Portland cement mortar).

2.2. Techniques and tests

The techniques and tests used in this study have been considered the most appropriate for the evaluation of the materials studied and are based on EN 17187: 2020 (40), allowing for further comparisons with mortars used in cultural heritage.

2.2.1. Petrographic, mineralogical, and chemical characterization

This study includes a series of complementary techniques and tests to characterize texturally and compositionally the four types of mortars studied. The petrographic study of the mortars from a macroscopic and microscopic point of view allows a visual description of the materials at different scales, highlighting the most influential textural and compositional characteristics in their physical-chemical behaviour.

For the macroscopic description (components, colour, appearance, consistency, porosity, etc.) a geologist's magnifying glass of x10 magnification was used. In addition, to check the visual level of carbonation (CaCO_3), a very alkaline pH indicator (phenolphthalein; EN 14630: 2006 (47)) was used. Microscopic description was carried out on 3x2 cm and 30 μm thin sections of each mortar with an OLYMPUS BX51 polarized light optical microscope (POM) with a 5 Mpx SC50 colour digital camera and Olympus CellSens Entry V2.3 image acquisition software.

A JOEL JSM-820 scanning electron microscope (SEM) with an energy dispersive X-ray spectroscopy (EDS) microanalyzer operating in back-scattered electron (BSE) mode was operated in vacuum conditions at a pressure of 0.50 torr and a voltage of 20 kV. An Oxford ISIS-Link acquisition, processing and analysis software was used to obtain higher accuracy and resolution. This equipment was used on the petrographic

analysis thin sections, previously coated with graphite (Cressington 108Carbon/A metallizer), to make them conductive to the electron beam. Semi-quantitative chemical microanalyses were performed on the binder mineral aggregates and zonal microanalyses on the binder matrix.

The crystalline mineral phases of the four mortars were detected by X-ray diffraction (XRD) on the powder fraction (< 53 µm) of 2 g total sample. The instrumental equipment was a BRUKER D8 diffractometer, with CuK α anode and graphite monochromator. The measurements were taken in a range between 2 and 65 [2θ], with an interval of 0.02 °/min in continuous mode.

Fourier transform infrared spectroscopy (FTIR) was used to determine the chemical structure of the inorganic components. For this test, 200 mg of BrK and 1.5 mg of the mortars powder samples were used. The equipment was a Nicolet Nexus 670-870 spectroscope measuring in the 4000-400 cm $^{-1}$ range of the infrared spectrum.

Thermogravimetry and differential thermal analysis (TG-DTA) were carried out to collect information at different temperatures on the processes occurring in the mortars studied (dehydration (< 200 °C), dehydroxylation (200-600 °C) y decarboxylation (600-900 °C)) and to interpret their carbonation and hydraulicity degrees (25, 36, 39, 48, 49). An SDT-Q600 equipment with UA software from TA Instruments and a nitrogen atmosphere with a flow rate of 100 ml/min and a heating up to 1000 °C at a speed of 10 °C/min was used. The amount of powder sample was 10-10.5 mg.

2.2.2. Petrophysical characterization

To determine the intrinsic characteristics of each type of mortar, different techniques and tests were implemented. These were divided into four large groups according to the qualities to be studied: 1-surface properties, 2-dynamic properties, 3-structural and hydric properties as well as 4-mechanical properties.

1-Surface properties: Tests which were carried out are listed as: 1) quantitative colour measurement (EN 15886: 2010 (50) and ASTM E313: 2020 (51)) using the parameters of the colour space CIE L*a*b* and a Minolta CM-700d/600D spectrophotometer with D65 illuminant and SpectraMagic NX Colour Data software (CM-100SW) as well as, 2) static contact angle measurement to evaluate the surface behaviour of the materials with respect to water (EN 15802: 2009 (52)) using a Dino-Lite Edge digital microscope model AM7915MZT, a x20-200 magnification and 5 MPx camera and a DinoCapture v2 software. Both tests were performed with a total of 3 measurements per sample on the larger prismatic specimens (10x10x4 cm).

2-Dynamic properties: Ultrasonic propagation velocity of P waves (V_p) (EN 14579: 2004 (53)) in the three spatial directions (X, Y, Z) of the 10x10x4 cm prismatic specimens were determined. Thus, 3 measurements per direction were taken with a Pundit CNS Electronics LTS portable ultrasound system with transducers of 1 MHz frequency and 1 cm diameter. Total anisotropy (dM, Equation [1]) was calculated, by using V_p in 3 directions of space. In addition, relative anisotropy (dm, Equation [2]) considering only the maximum and mean velocities of the materials, and the complete anisotropy (dMm=dM+dm) (54-56) were calculated.

$$dM(\%) = [1 - (2V_{p_{min}} / (V_{p_{mean}} + V_{p_{max}}))] \times 100 \quad [1]$$

$$dm(\%) = [(2 \times (V_{p_{max}} - V_{p_{mean}}) / (V_{p_{mean}} + V_{p_{max}}))] \times 100 \quad [2]$$

3-Structural and hydric properties: To define the internal structure of each type of mortar, tests to study the geometry and pore system distribution by the presence of fluids (mercury and water) were carried out.

By means of mercury intrusion porosimetry (MIP) (ASTM D4404: 2010 (57)), the percentage, size, and shape of the pores, as well as the porosity distribution in each type of mortar, were determined using 4 cylinders of 1.2x2 cm in size with 3 cm 3 in volume. Measurements were taken with a Micromeritics Autopore IV 9500 porosimeter.

To determine the hydric behaviour (fluid uptake, storage, and loss capacity), the following tests were carried out: 1) saturation test (EN 1936: 2006 (58)) on the 10x10x4 cm prismatic specimens, to determinate the real and apparent densities, the total and open porosities, the saturation and the compactness index, 2) water absorption test by immersion and water desorption test by evaporation at atmospheric pressure (EN 13755: 2008, NORMAL 7/81 (59, 60)) on the 10x10x4 cm prismatic specimens, 3) capillary water absorption test (EN 15801: 2009 (61)) on the 16x4x4 cm samples, 4) and water vapour permeability test (EN 15803: 2009 (62)) on the 5x5x1 cm square plates using the wet tray method (high humidity conditions, 93%). In addition, TinyPerm II portable air permeameter, was used on 10x10x4 cm prismatic specimens, to inject pressurized air into them for calculation of the absolute air permeability (K) in millidarcy (mD) using Equation [3], where T is the value obtained by the equipment.

$$T = -0.8206 - \log_{10}(K) + 12.8737 \quad [3]$$

4-Mechanical properties: For the estimation of the resistance to deformation or fracture under different stresses, mechanical tests were carried out on the 10×10×4 cm prismatic specimens. These are listed as follows: 1) the Leeb surface hardness test (HLD) or micro-rebound resistance test (EN ISO 16859-1: 2015 (63)), with the PROCEQ Equotip 3 equipment (impact energy of 11.5 Nmm (probe D) and 3 mm diameter tip to impact on binder), 2) the Schmidt surface hardness test (R) or rebound resistance test (ASTM D5873-14: 2023 (64)), using a PROCEQ Digi Schmidt 2000 model N digital sclerometer with an impact energy of 2.207 Nm and 1 cm diameter tip.

In addition, using the correlation of Deere and Miller (1966) (65), which uses the average rebound strength value of the Schmidt hammer and the bulk density of the materials, the indirect uniaxial simple compressive strength (UCS) was calculated using Equation [4]. This formula was used because of its high correlation ($R^2 = 0.94$) with similar materials (66) and this work will determine whether it is also reliable for use with mortars.

$$UCS(MPa) = 6.9 \cdot 10^{(0.0087 \cdot \rho \cdot R + 0.16)} \quad [4]$$

Obtained UCS values were compared with the hardness grade classification or international UCS values of the International Society for Rock Mechanics Commission (ISRM, (67)).

3. RESULTS AND DISCUSSION

3.1. Petrographic characterization

Macroscopically, all the mortars present a granular texture and a massive appearance, so their main differences are the colour and the cohesion between their aggregates and the binder (Figure 1). CL90-S PL is a white, not very dense, and nor competent mortar, which presents disaggregations or material losses on its surfaces as well as irregular pores and cracks. Whereas NHL2 and NHL5 are whitish-greyish mortars and dense and compact materials, also with rough surfaces. Their main differences are a higher cohesion between the aggregate and the binder and a lower porosity in NHL5 compared to NHL2. Finally, OPC has a greyish-greenish colour and a high density and hardness, as it is the only mortar with low porosity and smooth surfaces. Its porosity has a spheric morphology (vacuolar porosity), the same as in NHL2 and NHL5, but smaller in size.

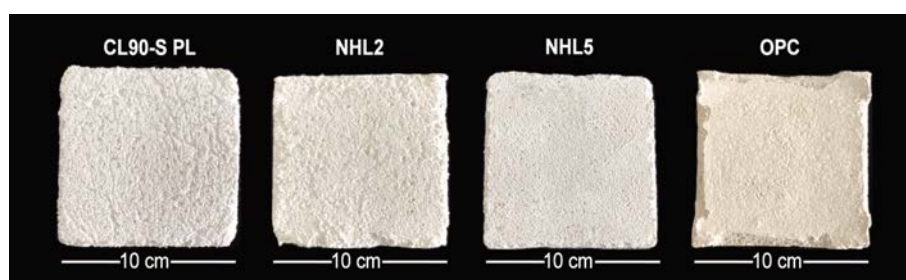


FIGURE 1. Macroscopic appearance of the mortars.

Optical microscopy (POM) shows that all the mortars present a granular texture dominated by inert siliceous aggregate (Figure 2). The aggregate is well selected and consisted of mono- and polycrystalline quartz grains of subangular to subrounded morphology with a grain size of 0.7 to 1.4 mm (coarse to very coarse sand).

In CL90-S PL, the binder consists of a microcrystalline mass which presents shrinkage cracks and fissures because of the curing (hardening process). Porosity of irregular morphology is also identified due to possible dissolution processes (Figures 2A-B). This binder is not carbonated (CaCO_3), as it presents low birefringence colours (grey colours in cross polarized light), which belong to portlandite (C-H , Ca(OH)_2) (Figure 2B).

In the binders of NHL2 and NHL5, concentrated masses of carbonate in the form of nodules and the increment of the birefringence colours in cross polarized light (ochre and brown, Figures 2D-F) are observed. This indicates the advance of the carbonation process, larger in NHL5 (2-3 cm depth). A greater chemical interaction between the binder and the aggregate is also seen in NHL5. The quartz grains show diffuse and sinuous edges, due to strong chemical reactions produced by the high pH ($\text{pH} > 10$, portlandite) reached during the hydration phase. Under these chemical conditions, the edges of the quartz grains dissolve ($\text{pH} > 9$), while the carbonates of the binder precipitate ($\text{pH} > 8$) on those edges. This allows the binder to adhere well to the aggregate, preventing its disintegration. It has been noted that in NHL2 there are some shrinkage cracks, not present in NHL5, and vacuolar porosity. This type of porosity, which is dominant in NHL5 (Figures 2C-D), is due to fluid bubbles trapped during mixing. NHL5 also shows more calcium silicates crystals than NHL2. These calcium silicates clusters appear poorly defined and have low birefringence in cross-polarized light mode (Figures 2E-F).

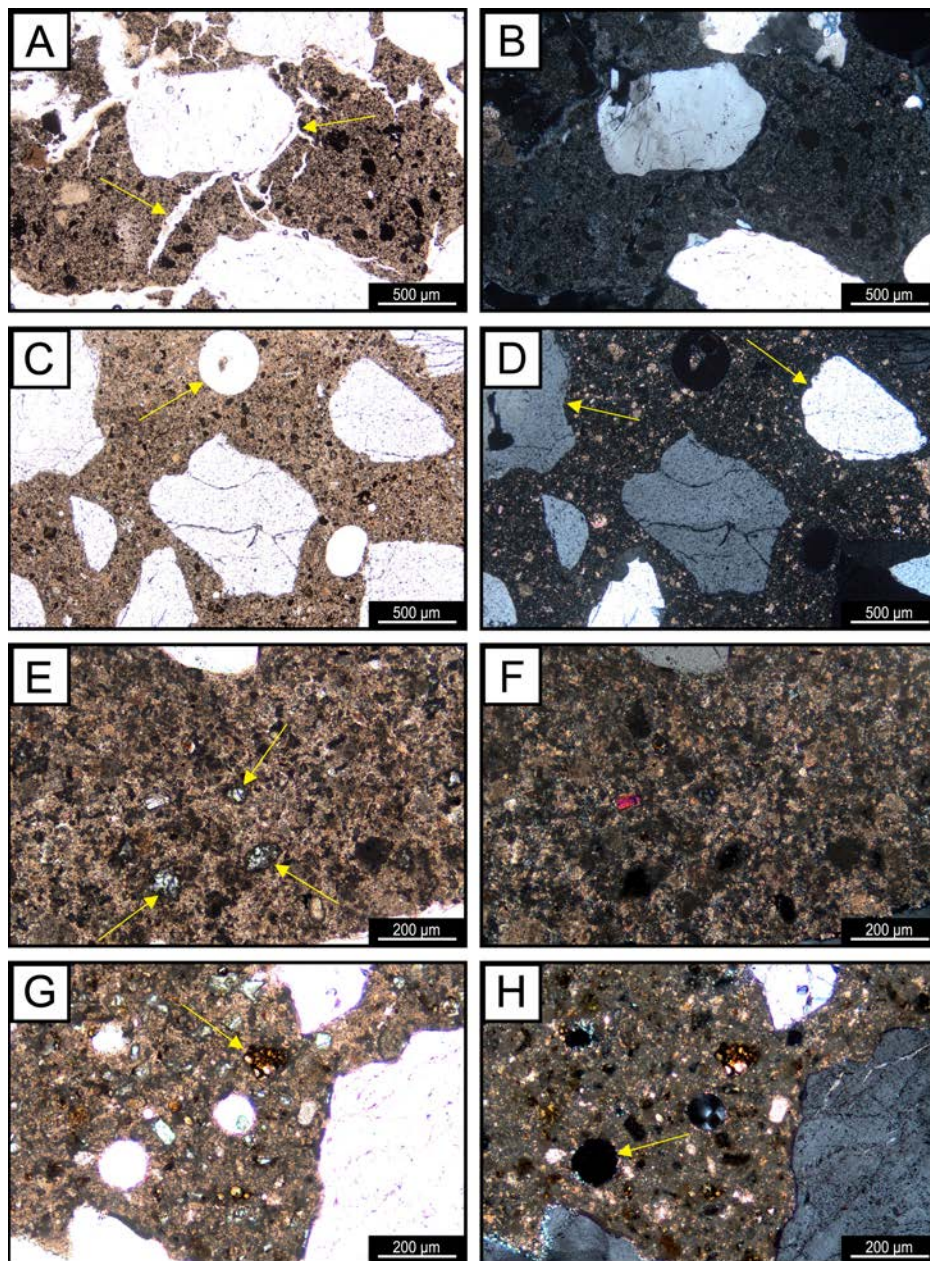


FIGURE 2. Polarized light optical microscope (POM) images, in parallel-polarized light (left) and cross-polarized light (right) of: CL90-S PL (A-B), NHL2 (C-D), NHL5 (E-F) and OPC (G-H). Marked by arrows in A: shrinkage cracks, in C and H: vacuolar porosity, in D: diffuse and sinuous edges of the aggregate grains, in E and G: calcium silicates clusters.

Lastly, OPC presents a heterogeneous binder with the most advanced degree of carbonation among all the studied mortars (highest birefringence throughout the thin section). This mortar also shows vacuolar porosity, quartz grains with very diffuse and dissolved edges and many calcium silicates clusters (hatrurite/alite - C_3S (Ca_3SiO_5) and larnite/belite - C_2S (Ca_2SiO_4), Figures 2G-H). These calcium silicates clusters appear well developed (70-180 μm), with various tones (alite - white and belite - brown, in parallel-polarized light), and sometimes also surrounded by ferruginous films (brownmillerite or calcium ferritoalumanite - C_2AF ($Ca_2(Al, Fe^{3+})_2O_5$) (Felite - C_4AF) (68, 69).

SEM results (Figure 3) confirm the observations made with POM. CL90-S PL presents a binder with a very homogeneous calcium composition (90-100% of CaO, by semi-quantitative EDS) and a lot of fissural porosity and microporosity (Figure 3A). The rest of the mortars, as they become more hydraulic, present in their binders more calcium silicates, carbonate nodules (95-100% of CaO) and vacuolar porosity (Figures 3B-D). In NHL2, monocalcium silicates (43% of SiO_2 and 57% of CaO ~ wollastonite - CS), bicalcium silicates (30-35% of SiO_2 and 60-65% of CaO ~ larnite/belite - C_2S) and some interstitial phases (20% of Fe_2O_3 , 20% of Al_2O_3 and 50% of CaO ~ brownmillerite - C_2AF) are abundant (Figure 3B). In NHL5 and OPC, tricalcium silicates (20-25% of SiO_2 and 70-75% of CaO ~ hatrurite/alite - C_3S) also appear (Figures 3C-D), although in greater proportion in OPC, in which monocalcium silicates (wollastonite) is no longer detected.

Regarding the chemical composition of the binder, it shows an enrichment in SiO_2 and Al_2O_3 in the more hydraulic mortars, as can be seen in the three-phase triangle (Figure 4, < 3% of SiO_2 and 1.5% of Al_2O_3 for CL90-S PL, 11-12% of SiO_2 and (2% of Al_2O_3 for NHL2, 20-21% of SiO_2 and ~ 5% of Al_2O_3 for NHL5 and 24-25% of SiO_2 and 7-8% of Al_2O_3 for OPC).

Thus, a series of characteristics related to the different degree of hydraulicity of the binders can be observed (Figure 5).

The higher the hydraulicity degree, the faster the carbonation, which explains that OPC, with well-developed tricalcium silicates (alite), has the most advanced degree of carbonation. It also be noted that as the hydraulicity degree increases, does the aggressiveness of the dissolution-precipitation chemical reactions at the edges of the aggregate, which are due to the alkaline nature of the surrounding binder (7).

Furthermore, water that is not able to react chemically with the components of the paste and that is used to increase the plasticity originates vacuolar pores, typical of hydraulic mortars. Natural hydraulic lime mortars (NHL2 and NHL5) differ in the degree of development of this type of porosity and in the aggressiveness of the alkaline reactions at the edges of the aggregate. Thus, the most hydraulic of them (NHL5) does not present shrinkage fissures, which impacts on a greater compactness and a less cohesion loss. Finally, CL90-S PL is the mortar that both micro and macroscopically shows the lowest degree of carbonation, which together with the high presence of shrinkage cracks results in high material losses or disaggregation.

In general, all lime mortars (especially CL90S-PL) do not show an advanced state of carbonation, which is explained by the curing time required by this type of materials (24, 70-72). This high portlandite/calcite ratio was also confirmed by XRD, FTIR and TG-DTA analysis.

Thus, Figure 6 shows that all mortars present peaks of portlandite (4.90Å) and calcite (3.03Å) of variable intensity depending on their state of hydration and carbonation, as well as high intensity peaks of quartz (3.34Å) due to the aggregate fraction.

After 90 days of curing, CL90-S PL shows the highest amount of portlandite (C-H), followed by NHL2, NHL5 and OPC. In CL90-S PL, in addition to calcite, one of its metastable polymorphs is also detected: aragonite (3.39Å, 3.27Å, 2.71Å). The presence of this mineral phase has been found very frequently in fresh mortars in which carbonation occurs at relative humidities similar to the curing conditions of this study (~ 60% RH) (48, 74, 75).

Regarding the characteristic phases of hydraulic binders (calcium silicates), they appear mainly in the range of 30-35° [2 θ] (2.98-2.56Å). Although they are difficult to detect because of the overlap between their peaks and those from the aggregate (Figure 6) (7, 48). The type of calcium silicates detected in all hydraulic binders is larnite/belite (C_2S), and only in OPC hatrurite/alite (C_3S) is also found. Larnite (2.79Å, 2.74Å and 2.33Å as distinctive peak) is the predominant hydraulic phase in natural hydraulic limes (76), as the most suitable temperatures for its formation are around 1000-1100 °C (77), the considered ones as optimal to produce this binder (78, 79).

On the other hand, hatrurite/alite is a characteristic mineral of higher hydraulicity binders, such as cement, that appears in the 32-33° [2 θ] range with their most distinctive peaks at 1.76 Å (51.8° [2 θ]) and 5.95Å (14.9° [2 θ]) (48). Although this type of calcium silicate can be also generated in natural hydraulic limes if there are "hot spots" (~ 1250 °C) in the kiln (80) during the calcination of the raw materials.

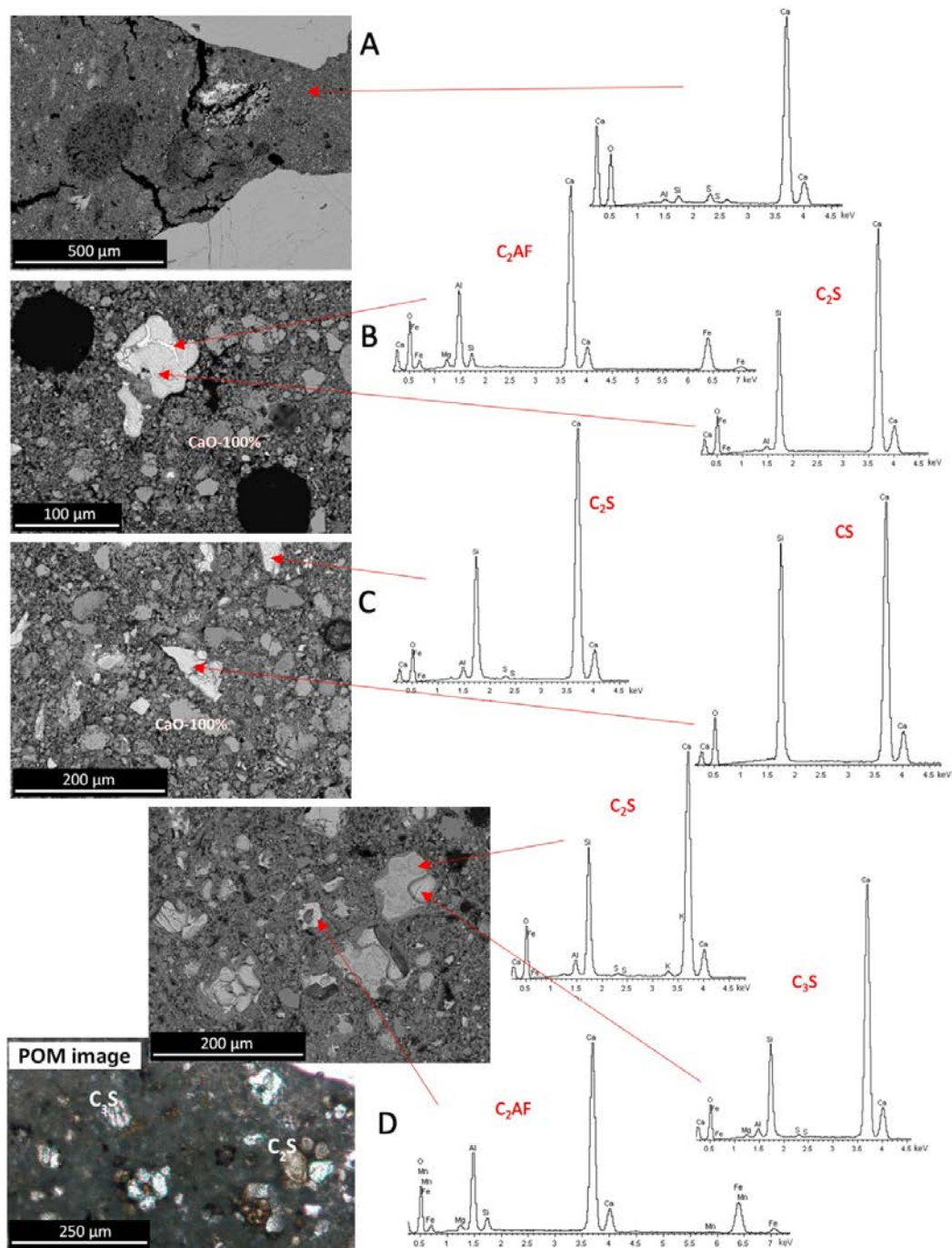


FIGURE 3. SEM images and EDS spectra of the binders of A) CL90-S PL, B) NHL2, C) NHL5, D) OPC. The presence of different calcium silicates stands out (wollastonite - CS, larnite/belite - C_2S , hatrurite/alite - C_3S , brownmillerite - C_2AF).

In addition, OPC presents other phases such as (Figure 6): calcium ferritoaluminates (brownmillerite or felite - 2.65\AA and 7.19\AA - $Ca_2(Al,Fe^{3+})_2O_5$) and calcium aluminates (celite - 2.69\AA - $Al_2O_3 \cdot 3CaO$; C_3A) (48, 81) as well as ettringite (9.16\AA ; $Ca_6Al_2(SO_4)_3(OH)_{12} \cdot 26H_2O$). It should be noted that the early/primary ettringite that precipitates in this system is not dangerous, although under site conditions (once the mortar has hardened and exposed to external agents: water, salts) it is susceptible to be transformed into delayed or secondary ettringite (82), which does give rise to expansion phenomena and the generation of gypsum (cracking, loss of mass and salt efflorescence pathologies) (83).

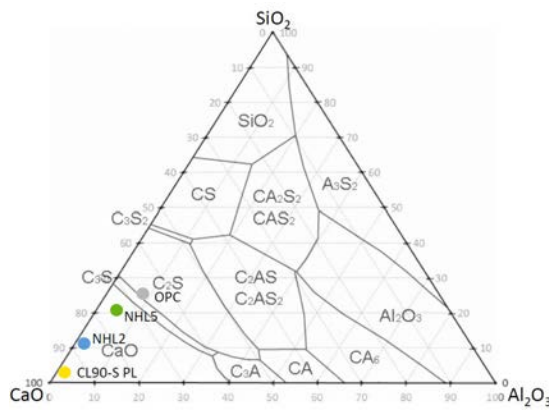


FIGURE 4. Ternary phase diagram of the CaO-SiO₂-Al₂O₃ system showing the four binders studied (modified from Taylor (32)).

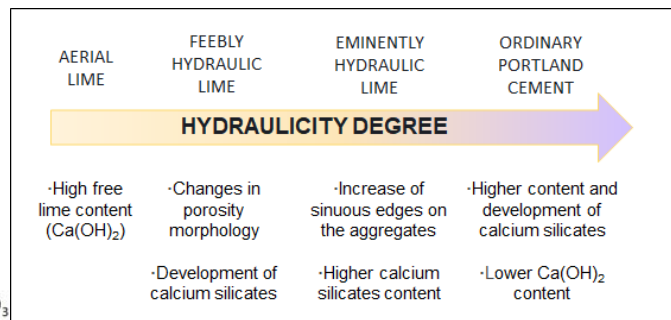


FIGURE 5. Diagram of the progression of the textural characteristics as the degree of hydraulicity increases.

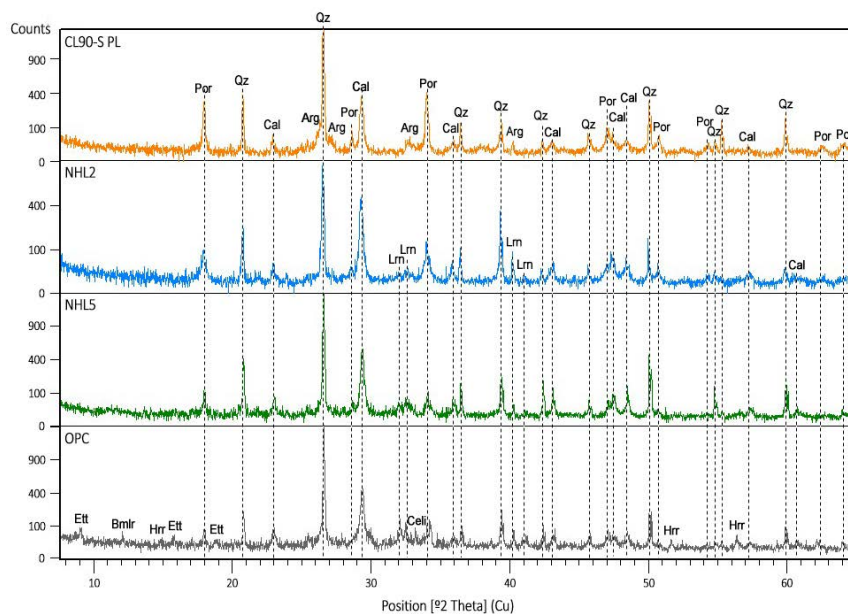


FIGURE 6. Diffractograms of the mortars studied in the range of 8 to 65 [°2θ].

Abbreviations according to Warr (2021) (73): Arg (Aragonite), Bmlr (Brownmillerite), Cal (Calcite), Ett (Ettringite), Hrr (Hatrurite-alite), Lrn (Larnite-belite), Por (Portlandite), Qz (Quartz). Celi: Celite.

Figure 7 shows the FTIR results. Thus, all mortars present a calcite stretching band domain (1450-1420 cm⁻¹) due to the carbonation process (CO₃²⁻) and an asymmetric stretching band at 1070-1080 cm⁻¹ because of the quartz aggregate (Si-O-Si). Portlandite (3640 cm⁻¹) appears with higher intensity in CL90-S PL and decreases progressively in NHL2 and NHL5 but is not present in OPC. It should also be noted that in CL90S-PL there are aragonite stretching (1470 cm⁻¹) and bending (855 cm⁻¹) bands due to the early carbonation process under high humidity conditions (CO₃²⁻).

In NHL2, NHL5 and OPC, the vibration bands of the quartz aggregate (1080-1190 cm⁻¹) mask the vibration bands of the calcium silicates. This causes them to appear to the right of the main quartz band (1070 cm⁻¹), at 990-1020 cm⁻¹, in the range reported in the literature (900-1120 cm⁻¹; (7, 48, 84, 85)). The bands at 990-1020 cm⁻¹ and 515-520 cm⁻¹ correspond mainly to belite/larnite (C₂S), while the alite vibration bands (C₃S), at 880-950 cm⁻¹ according to previous authors (48, 84, 85), are not detected.

The TG-DTA curves show four main weight loss regions: at < 120 °C, 120-200 °C, 200-600 °C and 600-900 °C (25, 36, 38, 39, 48, 49, 86). Table 1 shows the weight losses (%) in the different ranges.

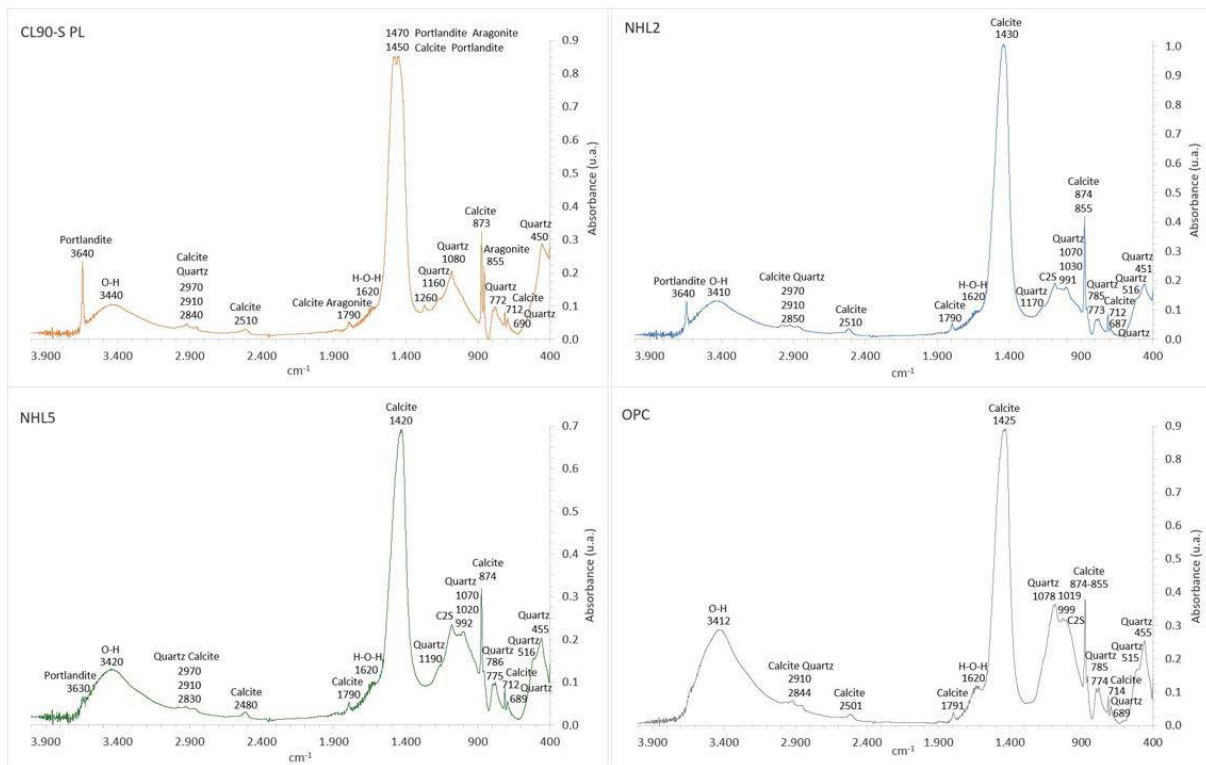


FIGURE 7. FTIR spectra of the mortars studied.

The weight loss at < 120 °C in all lime mortars (CL90-S PL, NHL2 and NHL5, < 3%) is due to the loss of water inside the mortars (T below 30 °C). While in OPC the dehydration of characteristic cement minerals such as ettringite and tobermorite (C-S-H) also occurs (weight loss of 3.7% at 70-75 °C, Table 1). Afterwards, in the range between 120 °C and 200 °C, in which the loss of crystallization water occurs, the weight loss of all the studied mortars is < 1%. These two ranges correspond to the dehydration phase of the samples (49, 86).

In the next region, at 200-600 °C, the weight loss is attributed to the loss of hydroxyl groups (dehydroxylation) (25, 36, 85-87) and specifically to the thermal decomposition of portlandite at 400-415 °C, which is the major component of the lime mortars (19-23% of loss), as well as OPC (17%).

Afterwards, the weight loss between 600 and 900 °C corresponds to the loss of CO₂ because of the decomposition of calcium carbonate, which enables the determination of the CaCO₃ content within the sample (decarboxylation) (25, 36, 87). In this way, all lime mortars (CL90-S PL, NHL2 and NHL5; 11-16%) present the highest loss percentages and OPC the lowest (~ 8%). Therefore, the total weight loss is higher in lime mortars (CL90-S PL, NHL2 and NHL5, 19-23%) than in OPC (17%) (Table 1).

Finally, the hydraulicity degree was calculated on the basis of the CO₂/H₂O ratio, so as this ratio decreases, the mortars are more hydraulic (25, 36, 39, 49); Table 1 and Figure 8).

TABLE I. Temperatures and weight loss (%) in the different TG-DTA analysis ranges.

	DEHYDRATION PHASE			DEHYDROXYLATION PHASE		DECARBOXYLATION PHASE		Total loss (%)	CO ₂ /H ₂ O (%)
	T (°C)	% of H ₂ O loss		T (°C)	% of OH loss at 200-600 °C	T (°C)	% of CO ₂ loss at 600-900 °C		
		< 120 °C	120-200 °C						
CL90-S PL	-	1.09	0.31	399.93	20.45	706.32	13.77	20.45	9.84
NHL2	27.96	2.28	0.54	401.01	23.44	714.63	15.51	23.44	5.50
NHL5	26.96	2.78	0.57	401.60	18.59	705.83	11.41	18.59	3.41
OPC	72.79	3.68	0.88	415.78	16.96	696.45	8.05	16.96	1.77

3.2. Petrophysical characterization

Surface properties: Colour is an important factor to consider, especially if mortars are going to be used on visible elements or facades. Based on the chromatic parameters, all the mortars are dull/matte (chroma $C^* < 6$, white-grey and a^* and b^* values close to zero, grey) with high lightness values ($L^* = 70-92$) and whiteness indexes (WI) greater than the yellowing ones (YI). CL90-S PL is the whitest mortar, followed by NHL2 and NHL5, while OPC is the most yellowish (Table 2). This is due to their mineralogy, in particular the presence of iron and aluminium phases such as brownmillerite in OPC and not in the lime mortars. Although there are other factors regarding the binders manufacturing process that impact on mortars colour, such as their raw materials composition and calcination temperatures.

The static contact angle test measurements provide information on the hydrophilic character of the mortars and therefore a first information on the behaviour of the mortar surface in relation to water.

Thus, CL90-S PL is classified as super-hydrophilic, that is, with a high affinity for water, as the droplet is quickly absorbed and not even the contact angle can be measured. While the rest of the mortars are hydrophilic, as they take longer to absorb the droplet and had $\theta < 90^\circ$. Therefore, the higher the hydraulicity of the binder and the droplet angle, the lower the hydrophilic character of the mortar. In consequence, OPC is the least hydrophilic mortar and presents the lowest standard deviation of all the mortars (Figure 9).

Dynamic properties: Table 3 shows the P-waves propagation values (V_p) of the mortars, which have a direct correlation with their hydraulic character.

On one hand, CL90-S PL and NHL2, as they present high porosities, shrinkage cracks and weak reactions between the paste and the aggregate, show an attenuation of the waves, presenting low V_p values (1258 m/s in CL90-S PL and 1352 m/s in NHL2). On the other hand, OPC presents a lower porosity and a higher density as well as cohesion, which impacts on V_p values > 3500 m/s. While NHL5, with characteristics in between, has V_p values of 1617 m/s, more similar to those of CL90-S PL and NHL2. Thus, the differences in V_p values between lime and cement mortars reflects their different setting and curing speed.

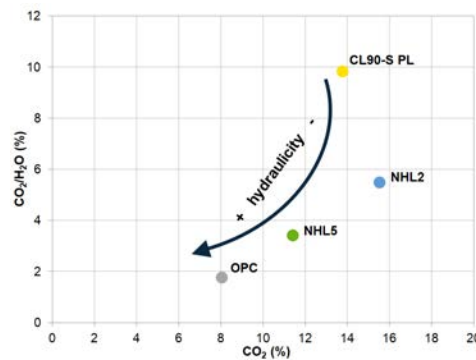


FIGURE 8. Graph of CO_2 (%) vs CO_2/H_2O (%) ratio of the mortars studied.

TABLE 2. Chromatic parameters of the mortars studied.

	L^*	a^*	b^*	C^*	WI	YI
CL90-S PL	91.76 ± 1.08	0.32 ± 0.11	3.54 ± 0.11	3.56 ± 0.11	62.61 ± 1.59	5.62 ± 0.11
NHL2	88.38 ± 0.81	0.48 ± 0.05	4.49 ± 0.33	4.51 ± 0.33	51.80 ± 2.90	7.34 ± 0.60
NHL5	87.44 ± 0.83	0.45 ± 0.08	5.27 ± 0.06	5.29 ± 0.06	46.62 ± 1.28	8.66 ± 0.10
OPC	73.41 ± 3.83	0.42 ± 0.07	5.91 ± 0.38	5.92 ± 0.39	26.10 ± 5.46	11.28 ± 1.19

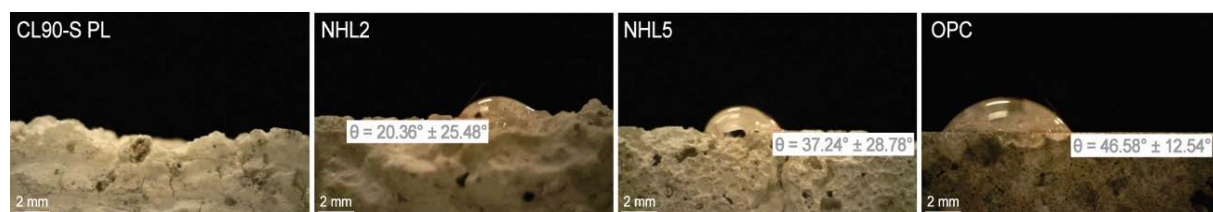


FIGURE 9. Average values of the droplet angle in the mortars studied.

TABLE 3. Mean values of P waves propagation velocity (Vp) and total (dM), relative (dm) and complete (dMm) anisotropies.

	Vp (m/s)	dM (%)	dm (%)	dMm (%)
CL90-S PL	1258.19 ± 24.12	2.39 ± 1.97	1.78 ± 1.63	4.17 ± 3.39
NHL2	1352.15 ± 20.68	15.41 ± 2.44	2.93 ± 1.88	18.34 ± 2.52
NHL5	1616.99 ± 23.06	5.08 ± 1.50	5.64 ± 2.89	10.72 ± 4.38
OPC	3542.68 ± 89.38	6.97 ± 4.51	0.69 ± 0.58	7.66 ± 4.03

Regarding the anisotropy, most of the mortars present a low complete anisotropy ($dMm < 10$) and similar total (dM) and relative anisotropy (dm) values. NHL2 and NHL5 are the most anisotropic mortars ($dMm > 10\%$), and NHL2 shows the most different values between dM and dm ($dM = 15.41\%$ and $dm = 2.93\%$), together with OPC ($dM = 6.97\%$ and $dm = 0.69\%$). The latter denotes the existence of preferential orientations in these mortars and, therefore, planes of structural weakness possibly due to the manufacturing process. By contrast, CL90-S PL ($dM = 2.39\%$ and $dm = 1.88\%$) is the least anisotropic mortar and shows a greater homogeneity.

Structural and hydric properties: Average values of the structural and hydric properties of the mortars studied are in Table 4. The real densities of all the mortars studied are high (~ 2460 - 2839 kg/m³ by MIP), and higher than their bulk densities (~ 1492 - 2026 kg/m³ by saturation), showing the presence of important percentages of porosity. Furthermore, the real and bulk density values obtained by MIP and by saturation are similar in most of the mortars, even though they were performed with different fluids and in different mortar samples.

TABLE 4. Average values of the structural and hydric properties studied.

	CL90-S PL	NHL2	NHL5	OPC	
Real density (kg/m ³) by MIP	2480.8	2838.8	2459.8	2509.6	
Real density (kg/m ³) by saturation	2543.56 ± 5.94	2596.76 ± 1.66	2629.99 ± 1.97	2644.73 ± 7.90	
Bulk density (kg/m ³) by MIP	1567.2	1759.1	1615.1	2004.2	
Bulk density (kg/m ³) by saturation	1491.96 ± 10.78	1612.72 ± 8.50	1605.85 ± 6.03	2025.67 ± 5.41	
Total porosity (%) by MIP	36.83	38.03	34.34	20.14	
Total porosity (%) by saturation	41.46 ± 0.44	38.02 ± 0.29	39.06 ± 0.26	23.56 ± 0.37	
Open porosity (%)	41.34	37.89	38.94	23.41	
Pore geometry	Specific pore surface area (m ² /g)	3.54	6.62	9.71	8.92
	Average pore diameter (μm)	0.27	0.13	0.09	0.05
Average pore size (μm)	0.53	0.79	1.13	0.36	
Pore size distribution (%)	Microporosity	66.8	93.6	95.7	96.9
	Macroporosity	33.2	6.4	4.3	3.1
Tortuosity	4.91	8.15	2.86	3.10	
Compactness index (0-1)	0.59	0.62	0.61	0.76	
Saturation (%)	27.71 ± 0.49	23.50 ± 0.30	24.25 ± 0.25	11.56 ± 0.21	
Water absorption coefficient at P _{atm} (%)	23.64 ± 0.37	21.62 ± 0.47	21.81 ± 0.18	10.49 ± 0.07	
Capillary absorption coefficient (kg/m ² ·s ^{0.5})	0.15427 ± 0.00948	0.16193 ± 0.02474	0.15276 ± 0.03060	0.03540 ± 0.01001	
Water vapour permeability coefficient (kg/m·s·Pa)	9.04·10 ⁻⁹ ± 1.47·10 ⁻⁹	4.37·10 ⁻⁹ ± 3.43·10 ⁻¹⁰	4.30·10 ⁻⁹ ± 2.73·10 ⁻¹¹	2.17·10 ⁻⁹ ± 4.41·10 ⁻¹⁰	
Water vapour flow rate (kg/s)	9.58·10 ⁻⁹ ± 1.71·10 ⁻⁹	4.58·10 ⁻⁹ ± 2.03·10 ⁻¹⁰	4.42·10 ⁻⁹ ± 2.47·10 ⁻¹⁰	2.63·10 ⁻⁹ ± 6.34·10 ⁻¹⁰	
Water vapour transmission rate (kg/s·m ²)	5.52·10 ⁻⁶ ± 9.87·10 ⁻⁷	2.64·10 ⁻⁶ ± 1.17·10 ⁻⁷	2.55·10 ⁻⁶ ± 1.42·10 ⁻⁷	1.52·10 ⁻⁶ ± 3.65·10 ⁻⁷	
Water vapour penetration (kg/m ² ·s·Pa)	6.09·10 ⁻⁷ ± 1.09·10 ⁻⁷	2.91·10 ⁻⁷ ± 1.29·10 ⁻⁸	2.81·10 ⁻⁷ ± 1.57·10 ⁻⁸	1.67·10 ⁻⁷ ± 4.03·10 ⁻⁸	
Air permeability (mD)	3717.00 ± 0.17	-	-	-	

In terms of total porosities by both PIM and saturation, all lime mortars (CL90-S PL, NHL2 and NHL5) have a porosity of around 40%, while in OPC it is half that (~ 20%). The highest percentages correspond to open porosity and Figure 10 shows the distribution curves of the different pore sizes of each mortar. In it, it has been noted that all the mortars are microporous (< 5 µm), with average pore sizes of 0.4 to 1.1 µm, and that the most microporous ones (94-97%) are the hydraulic mortars (NHL2, NHL5 and OPC). It should be noted that microporous mortars may tend to degrade if they have a low desorption capacity, as salts may precipitate inside them and the harmful effects are very difficult to detect, but very aggressive.

All the mortars studied have at least 3 pore-size populations in the microporosity range (0.01-0.1 µm, 0.1-1 µm and 1-3 µm, Figure 10) with average pore sizes between 0.36 µm and 1.13 µm depending on the mortar (Table 4).

The most remarkable intervals in NHL2, NHL5 and OPC are 0.1-1 µm and 1-3 µm, whereas CL90-S PL, in line with its appearance, presents a high percentage of macroporosity (> 5 µm, at least 1/3 of its total porosity). However, the value of the average pore size of CL90S-PL (0.36 µm) is lower than the actual average size, as the PIM technique does not consider pore sizes larger than 300 µm.

The mortars percentages of porosity are in relation to their compactness indexes (Table 4), around 0.6 in all lime mortars (CL90-S PL, NHL2 and NHL5) and 0.8 in OPC, the most dense and compact material.

Concerning the shapes of the pores, due to their large specific surfaces and small diameters (Table 4), all the mortars, especially the most hydraulic (NHL5 and OPC), have irregular pores and low (< 10) tortuosity values (capillary connections). This indicates straight connections that facilitate water ingress, so none of the mortars seem to offer water resistance, as previously verified by the static contact angle test. It also affects their water saturation capacity, absorption, desorption, capillary suction, and permeability.

As a result of the saturation test (Table 4), all lime mortars present similar values (28% of saturation in CL90-S PL and 24% in NHL2 and NHL5), whereas OPC has the lowest percentage of saturation (12%). This trend, in which lime mortars have a similar hydric behaviour while OPC does not, is also observed in the rest of the hydric tests.

First, during the water absorption test (Figure 11), all samples experience 90% water absorption in the first minutes. Their absorption coefficients are 24% (CL90-S PL), 22% (NHL2 and NHL5) and 11% (OPC). Thus, all lime mortars have a high absorption capacity, while it is the desorption phase that makes the difference between aerial and hydraulic mortars.

The CL90-S PL samples eliminate all their water content in approximately 24 hours, whereas the hydraulic mortars, and especially OPC, show a more distended desorption slope (much slower water loss) and leave a percentage of water retained inside. At the end of the test, NHL2 samples retain ~ 25% absorbed water, NHL5 ~ 35%, and OPC ~ 50% (Figure 11).

In the second place, during the capillary test, the lime mortars (CL90-S PL, NHL2 and NHL5) show a similar behaviour to the absorption test. The trend of their curves and their capillary absorption coefficients are different from those of OPC (Figure 12, Table 4). Thus, OPC absorbs up to 3 times less water than the lime mortars at the end of the test and shows a much slower and more distended absorption over time. OPC presents averages of 15.55 kg/m² of water per unit area, whereas the lime mortars have much steeper slopes and absorb the largest amounts of water (50.94 kg/m² - CL90-S PL, 56.18 kg/m² - NHL2, and 50.44 kg/m² - NHL5). The capillary absorption coefficients range from 0.15-0.16 kg/m²·s^{0.5} in lime mortars to (0,04 g/m²·s^{0.5} in OPC (Table 4), which is a significant difference regardless of the degree of hydraulicity of the limes.

Finally, the higher the hydraulicity, the lower the water vapour permeability of the mortars, which is directly related to the porosity (pore shape, average pore size, size distribution and capillary connections) (Table 4). CL90-S PL is the most permeable mortar (9.04·10⁻⁹ kg/m·s·Pa) with the highest values of water vapour flow rate, transmission rate and water vapour penetration, while NHL2 and NHL5 are half as permeable than CL90-S PL (4.37·10⁻⁹ and 4.30·10⁻⁹ kg/m·s·Pa). OPC is up to four times less permeable (2.17·10⁻⁹ kg/m·s·Pa) than CL90-S PL and half as permeable as NHL2 and NHL5.

Therefore, the only mortar sufficiently air permeable to perform the measurement with the air permeameter was CL90-S PL, which obtained a value of 3717 mD on average because of its high macroporosity (Table 4).

Mechanical properties: The mortars with the highest degree of hydraulicity show the highest hardness values after 90 days of curing (Table 5). In all cases, OPC doubles the hardness and strength of NHL2 and NHL5 and triples those of CL90-S PL, being the most suitable material for high mechanical stresses.

Thus, CL90-S PL shows the lowest values of Schmidt hardness (7 R) and microhardness (Leeb hardness, 213 HLD), while NHL2 and NHL5 present hardnesses of 18-20 R and microhardnesses of 260-267 HLD, although they are also classified as relatively soft materials. OPC, as expected, has the highest values with moderate micro-rebound (~ 428 HLD) and rebound (~ 30 R) resistance.

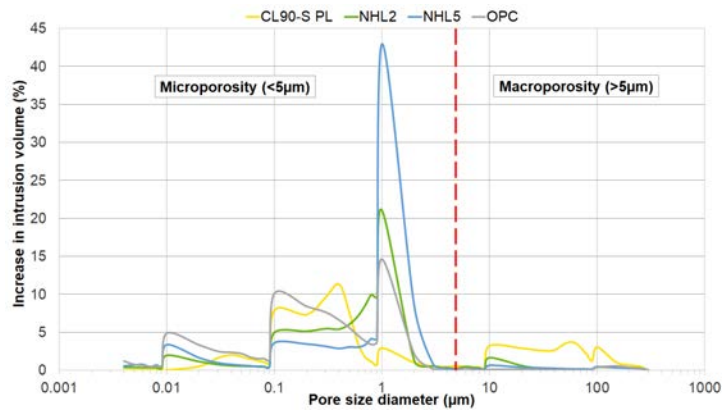


FIGURE 10. Pore size distribution curves. The red line marks the limit between microporosity and macroporosity.

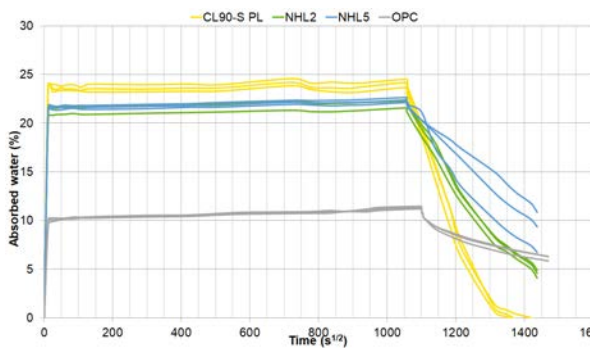


FIGURE 11. Kinetic curves of water absorption-desorption at atmospheric pressure.

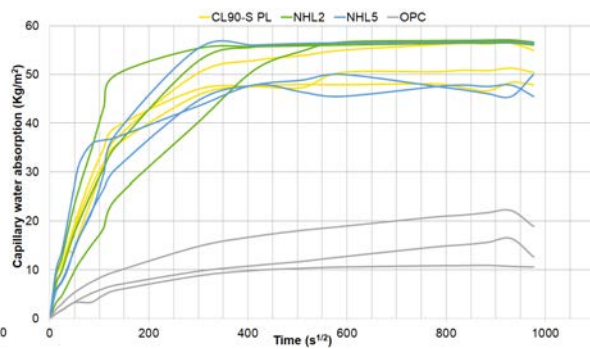


FIGURE 12. Capillary absorption curves.

TABLE 5. Results obtained in the different mechanical tests.

	Leeb hardness (HLD)	Schmidt hardness (R)	UCS (MPa)
CL90-S PL	212.8 ± 26.5	7.33 ± 6.35	12.56 ± 2.24
NHL-2	267.0 ± 56.7	17.67 ± 3.51	17.72 ± 1.99
NHL-5	260.4 ± 35.8	19.77 ± 1.53	18.85 ± 0.91
OPC	427.8 ± 52.5	30.27 ± 3.59	34.31 ± 5.18

Finally, the calculated UCS values (Table 5) for the lime mortars (CL90-S PL ~ 13 MPa, NHL2 ~ 18 MPa and NHL5 ~ 19 MPa) were equivalent in strength to a soft stone (5-25 MPa) and for the OPC (~ 34 MPa) to a moderately hard stone (25-50 MPa).

In the case of CL90-S PL its UCS values are due to its high disintegration capacity, incomplete carbonation state and high porosity and cracking. NHL2 and NHL5 exhibit similar hardness and UCS values due to their porosity characteristics and slight-moderate chemical reactions. And the high values of OPC are mainly due to their higher curing speed (higher degree of carbonation) and lower porosity, in addition to the strong chemical reactions between the aggregate and the binder.

4. CONCLUSIONS

After a curing period of 90 days, all the mortars, especially the lime mortars (aerial and hydraulic), do not complete their carbonation process. The results of the petrographic and petrophysical techniques showed clear differences between lime and cement mortars.

Thus, in the air lime mortar a high content of free lime (Ca(OH)₂) is detected, whereas in hydraulic mortars, it decreases. In hydraulic mortars there is a development of hydraulic phases, changes in the porosity morphology (high vacuolar porosity) and more aggressive alkaline reactions as the hydraulicity of the binder increases.

In terms of their petrophysical properties, all lime mortars (CL90-S PL, NHL2 and NHL5) present high porosities (34-41%), being twice as high as the porosity of the cement mortar (OPC, 20-23%). This results in lower P-waves propagation velocities in lime mortars (< 2000 m/s) and > 3500 m/s in OPC.

The high porosity of the lime mortars also results in high water absorption, desorption, saturation and capillary rise capacities. In consequence, the hydric values of CL90-S PL, NHL2 and NHL5 are three to two times higher than those of cement mortar, while their hardness and strength are lower (7-20 R and 13-19 MPa) than those of OPC (30 R, ~ 34 MPa). The evolution of strength and the acquisition of higher hardness in lime mortars can take years, which represents its greatest weakness as a building material.

In this sense, the air lime mortar (CL90-S PL) is the most porous and hydrophilic material. It presents up to 33% of macroporosity (> 5 µm) as well as cracks and fissures that affect its binder, which together with its incomplete setting process causes intergranular disaggregations. In addition, the slightly sinuous shape of its pores favours its water vapour permeability, as well as its air permeability.

Given its petrophysical properties, the most suitable use of this material shall be recommended for restoration or coating works in dry climates, in environments with low humidity or in construction elements that do not require high mechanical stresses.

On the other hand, the cement mortar (OPC) is the hardest, densest and most competent material due to its advanced state of carbonation, as it was the only mortar that rapidly reached this state. This material doubles the hardness and strength of lime mortars with strength values similar to those of a moderately hard stone. Mineralogically, it has a high content of hydraulic phases (C₂S-larnite/belite and C₃S-hatruirite/alite), as well as aluminous phases such as C₃A-celite, C₂AF-brownmillerite and ettringite (hydrated Al-Ca sulphate that can give rise to deterioration pathologies if transformed into secondary ettringite).

Furthermore, it should be noted that the cement mortar is the least porous and hydrophilic of all mortars. The latter is related to its high microporosity (97%), average pore size (< 5 µm) and very sinuous pore morphology, which does not favour its water behaviour, nor its permeability to air or water vapour.

In fact, the disadvantages of cement mortar as a building material are its high stiffness and impermeability, the recognised presence of harmful compounds (gypsum and alkalis) and its microporosity with long water retention times that can favour dampness, a vehicle for associated pathologies such as *sanding* and efflorescence).

Finally, natural hydraulic lime mortars (NHL2 and NHL5) present petrographic characteristics similar to each other and to OPC, as they all present calcium silicates (with variable complexity depending on their hydraulic degree) and vacuolar porosity. In contrast, NHL mortars show similar petrophysical and mechanical properties to air lime mortar (CL90-S PL) due to their high porosity (34-39%), which favours their absorption, desorption and saturation of water, as well as their capillary rise. In addition, it should be noted that the high microporosity (94-96%) and sinuous morphology of their pores (similar to OPC), influence their water vapour permeability values (half that of CL90-S PL and double that of OPC), as well as their low strength and hardness.

For all stated reasons above, the most suitable function of NHL mortars shall be for elements or structures in contact with high humidity and not subjected to high stresses. In particular, the NHL2 mortar shall be recommended as cladding mortar in order to take advantage of its less mechanical requirements and high permeability and porosity (physical-mechanical properties similar to air lime).

Thus, the combination of petrographic and petrophysical techniques used in the EN 17187 (2020) standard (40), especially POM, SEM+EDS and XRD, as well as the hydric tests, has made it possible to characterize and highlight the most distinctive aspects of each of the four types of mortars studied.

Acknowledgements

The authors would like to acknowledge the Research Group 921349 of the Complutense University of Madrid and the professional support of the Interdisciplinary Thematic Platform from CSIC Open Heritage: Research and Society (PTI-PAIS).

Funding Sources

This work has been funded within the project TOP-HERITAGE-Technologies in Heritage Sciences (S2018/NMT-4372) of the Community of Madrid.

Clara Parra-Fernández is a PhD student under the FPI grant of the Ministry of Science and Innovation and the State Research Agency of Spain (PRE2021-098699).

Authorship contribution statement

Clara Parra-Fernández: Data curation, Formal analysis, Investigation, Methodology, Software, Validation, Visualization, Writing - original draft, Writing - review & editing.

María Josefa Varas Muriel: Conceptualization, Formal analysis, Funding acquisition, Investigation, Project administration, Resources, Supervision, Writing - original draft, Writing - review & editing.

Declaration of competing interest

The authors of this article declare that they have no financial, professional or personal conflicts of interest that could have inappropriately influenced this work.

REFERENCES

1. Martínez-Ramírez S, Blanco-Varela MT. 2012. Caracterización de morteros históricos. Programa Geomateriales (Ed), La conservación de los geomateriales utilizados en el patrimonio, 55-62.
2. Lancaster LC. 2021. Mortars and plasters-How mortars were made. The literary sources. *Archaeol. Anthropol. Sci.* 13(11):192. <https://doi.org/10.1007/s12520-021-01395-0>
3. Varas MJ, Álvarez de Buergo M, Fort R. 2007. Piedras artificiales: morteros y hormigones. El cemento como máximo representante de estos materiales de construcción. Ayuntamiento de San Sebastián de los Reyes (Ed), Ciencia Tecnología y Sociedad para una conservación sostenible del patrimonio pétreo, 179-189.
4. Arizzi A, Cultrone, G. 2021. Mortars and plasters-how to characterize hydraulic mortars. *Archaeol. Anthropol. Sci.* 13:144. <https://doi.org/10.1007/s12520-021-01404-2>
5. Sersale R. 1991. Lime: the first intimate among the justly named binding materials. *Atti della Accademia pontaniana*, 40:257-275.
6. Alejandro Sánchez FJ. 2002. Historia, caracterización y restauración de morteros, Universidad de Sevilla: Secretariado de publicaciones, Instituto Universitario de Ciencias de la Construcción. <http://doi.org/10.12795/9788447221813>
7. Varas MJ, Álvarez de Buergo M, Fort R. 2005. Natural cement as the precursor of Portland cement: Methodology for its identification. *Cem. Concr. Res.* 35(11):2055-2065. <https://doi.org/10.1016/j.cemconres.2004.10.045>
8. Varas MJ, Álvarez de Buergo M, Fort R. 2007. The origin and development of natural cements: The Spanish experience. *Constr. Build. Mater.* 21(2):436-445. <https://doi.org/10.1016/j.conbuildmat.2005.07.011>
9. European Committee for Standardization (Comité Européen de Normalisation, CEN). EN 459-1. 2015. Building lime - Part 1: Definitions, specifications and conformity criteria.
10. Cowper AD. 1927. Lime and lime mortars. Donhead Publishing Ltd. Shaftesbury (UK).
11. Mertens G, Lindqvist JE, Sommain D, Elsen J. 2008. Calcareous hydraulic binders from a historical perspective. In Proceedings I of the Historical Mortar Conference (HMC08), 1-15, Lisbon, Portugal.
12. Eckel EC. 1922. Cement, limes and plasters: their materials, manufacture and properties, Wiley, London.
13. Oates JAH. 1998. Lime and limestone. Chemistry and technology, production and uses. First edition, Wiley-VCH, Weinheim.
14. Mertens G. 2009. Characterisation of historical mortars and mineralogical study of the physico-chemical reactions on the pozzolan-lime binder interface. PhD Thesis, Catholic University of Leuven.
15. Collepardi M. 1990. Degradation and restoration of masonry walls of historical buildings. *Mater. Struct.* 23(2):81-102. <https://doi.org/10.1007/BF02472568>
16. Penazzi D, Valluzzi MR, Cardani G, Binda L, Baronio G, Modena C. 2000. Behaviour of historic masonry buildings in seismic areas: lessons learned from the Umbria-Marche earthquake. In Proceedings 12th International Brick and Block Masonry Conference, Volume I, 217-235, Madrid, Spain.
17. Callebaut K, Elsen J, Van Balen K, Viaene W. 2001. Nineteenth century hydraulic restoration mortars in the Saint Michael's Church (Leuven, Belgium): Natural hydraulic lime or cement? *Cem. Concr. Res.* 31(3):397-403. [https://doi.org/10.1016/S0008-8846\(00\)00499-3](https://doi.org/10.1016/S0008-8846(00)00499-3)
18. Álvarez J, Lanás J. 2006. Preparación y ensayos de morteros de cal de nueva factura para su empleo en restauración del patrimonio. V Jornada Técnicas de Restauración y Conservación del Patrimonio, 1-13, La Plata, Argentina.
19. Mileto C, Vegas López-Manzanares F, García-Soriano L. 2017. La restauración de la tapia monumental: pasado, presente y futuro. *Inf. Constr.* 69(548):e231. <https://doi.org/10.3989/ic.16.160>
20. Kirilovica I, Vitina I, Lindina L. 2018. Hydration of cement minerals in a hydraulic dolomitic binder. *Key Eng. Mater.* 762:356-361. <https://doi.org/10.4028/www.scientific.net/KEM.762.356>
21. Adams J, Dollimore D, Griffiths DL. 1993. Thermal analysis investigation of ancient mortars from Gothic structures. *J. Therm. Anal.* 40:275-284. <https://doi.org/10.1007/bf02546578>
22. Giavarini C, Ferretti AS, Santarelli ML. 2006. Mechanical characteristics of Roman "opus caementicium". In S. K. Kourkoulis (Ed.), *Fracture and Failure of Natural Building Stones*, Berlin: Springer, 107-120. https://doi.org/10.1007/978-1-4020-5077-0_7
23. Moropoulou A, Bakolas A, Bisbikou K. 2000. Investigation of the technology of historic mortars. *J. Cult. Herit.* 1(1):45-58. [https://doi.org/10.1016/S1296-2074\(99\)00118-1](https://doi.org/10.1016/S1296-2074(99)00118-1)

24. Zhang D, Zhao J, Wang D, Xu C, Zhai M, Ma X. 2018. Comparative study on the properties of three hydraulic lime mortar systems: Natural hydraulic lime mortar, cement-aerial lime-based mortar and slag-aerial lime-based mortar. *Constr. Build. Mater.* 186:42-52. <https://doi.org/10.1016/j.conbuildmat.2018.07.053>
25. Ergenç D, Fort R, Varas-Muriel MJ, Álvarez de Buergo M. 2021. Mortars and plasters-How to characterize aerial mortars and plasters. *Archaeol. Anthropol. Sci.* 13:197. <https://link.springer.com/article/10.1007/s12520-021-01398-x>
26. Van Balen K. 2005. Carbonation reaction of lime, kinetics at ambient temperature. *Cem. Concr. Res.* 35(4):647-657. <https://doi.org/10.1016/j.cemconres.2004.06.020>
27. Forsyth M. 2008. *Materials & skills for historic building conservation*. Blackwell Publishing Ltd. <https://doi.org/10.1002/9780470697696>
28. Cizer Ö, Schueremans L, Serre G, Janssens E, Van Balem K. 2010. Assessment of the compatibility of repair mortars in restoration projects. *Adv. Mater. Res.* 133-134:1071-1076. <https://doi.org/10.4028/www.scientific.net/AMR.133-134.1071>
29. Schueremans L, Cizer Ö, Janssens E, Serre G, Balen KV. 2011. Characterization of repair mortars for the assessment of their compatibility in restoration projects: Research and practice. *Constr. Build. Mater.* 25(12):4338-4350. <https://doi.org/10.1016/j.conbuildmat.2011.01.008>
30. Henry A, Stewart J. 2011. *Mortars, renders & plasters*. English Heritage, Practical Building Conservation, Ashgate Publishing Limited, Farnham.
31. Figueiredo C, Lawrence M, Ball RJ. 2016. Chemical and physical characterisation of three NHL 2 binders and the relationship with the mortar properties. In *REHABEND 2016, Euro-American Congress: Construction Pathology, Rehabilitation Technology and Heritage Management, 1293-1300*, Burgos, España.
32. Taylor HFW. 1998. *Cement chemistry*. Second edition. Thomas Telford. London.
33. Cultrone G, Sebastián Pardo E, Ortega Huertas M. 2005. Forced and natural carbonation of lime-based mortars with and without additives: Mineralogical and textural changes. *Cem. Concr. Res.* 35(12):2278-2289. <https://doi.org/10.1016/j.cemconres.2004.12.012>
34. Arizzi A, Cultrone G. 2014. The water transfer properties and drying shrinkage of aerial lime-based mortars: An assessment of their quality as repair rendering materials. *Environ. Earth. Sci.* 71(4):1699-1710. <https://doi.org/10.1007/s12665-013-2574-x>
35. Feilden BM. 2003. *Conservation of historic buildings*. Third edition, Architectural Press, Oxford.
36. Moropoulou A, Bakolas A, Anagnostopoulou S. 2005. Composite materials in ancient structures. *Cem. Concr. Compos.* 27(2):295-300. <https://doi.org/10.1016/j.cemconcomp.2004.02.018>
37. Varas-Muriel MJ, Pérez-Monserrat EM, Vázquez-Calvo MC, Fort R. 2015. Effect of conservation treatments on heritage stone. Characterisation of decay processes in a case study. *Constr. Build. Mater.* 95:611-622. <https://doi.org/10.1016/j.conbuildmat.2015.07.087>
38. Ponce-Antón G, Cruz Zuluaga M, Ortega LA, Agirre Mauleon J. 2020. Petrographic and chemical-mineralogical characterization of mortars from the Cisterna at Amaiur Castle (Navarre, Spain). *Minerals.* 10(4):311. <https://doi.org/10.3390/min10040311>
39. Fort R, Varas-Muriel MJ, Zoghalmi K, Ergenç D, Zaddem A. 2024. Analytical characterisation of 1st- and 2nd-century Roman mortars at the Utica archaeological site (Tunisia): construction phases and provenance of the raw materials. *J. Archaeol. Sci. Rep.* 54:104404. <https://doi.org/10.1016/j.jasrep.2024.104404>
40. European Committee for Standardization (Comité Européen de Normalisation, CEN). EN 17187. 2020. Conservation of cultural heritage - Characterization of mortars used in cultural heritage.
41. European Committee for Standardization (Comité Européen de Normalisation, CEN). EN 197-1. 2011. Cement - Part 1: Composition, specifications and conformity criteria for common cements.
42. Ministerio de Fomento. Secretario General Técnico. Comité Permanente del Cemento. RC-16. 2016. Instrucción para la recepción de cementos.
43. Veiga MR, Aguiar J, Silva AS, Carvalho F. 2001. Methodologies for characterisation and repair of mortars of ancient buildings. In *Proceedings of the 3rd International Seminar Historical Constructions: possibilities of numerical and experimental techniques*, 353-362, Guimarães, Portugal.
44. Grilo J, Silva AS, Faria P, Gameiro A, Veiga R, Velosa A. 2014. Mechanical and mineralogical properties of natural hydraulic lime-metakaolin mortars in different curing conditions. *Constr. Build. Mater.* 51:287-294. <https://doi.org/10.1016/j.conbuildmat.2013.10.045>
45. Pavlík V, Užáková M. 2016. Effect of curing conditions on the properties of lime, lime-metakaolin and lime-zeolite mortars. *Constr. Build. Mater.* 102(1):14-25. <https://doi.org/10.1016/j.conbuildmat.2015.10.128>
46. Santhanam K, Ramadoss R. 2022. Sustainability development and performance evaluation of natural hydraulic lime mortar for restoration. *Environ. Sci. Pollut. Res. Int.* 29(6):79634-79648. <https://doi.org/10.1007/s11356-022-21019-x>
47. European Committee for Standardization (Comité Européen de Normalisation, CEN). EN 14630. 2006. Products and systems for the protection and repair of concrete structures - Test methods - Determination of carbonation depth in hardened concrete by the phenolphthalein method.
48. Trezza MA, Scian AN. 2013. Aporte de las técnicas ATD/TG y espectroscopía FT-IR al estudio de la carbonatación de la matriz cementicia. *Afinidad LXX*, 562:112-117.

49. Borsoi G, Santos Silva A, Menezes P, Candeias A, Mirão J. 2019. Analytical characterization of ancient mortars from the archaeological roman site of Pisões (Beja, Portugal). *Constr. Build. Mater.* 204:597-608. <https://doi.org/10.1016/j.conbuildmat.2019.01.233>
50. European Committee for Standardization (Comité Européen de Normalisation, CEN). EN 15886. 2010. Conservation of cultural property - Test methods - Colour measurement of surfaces.
51. American Society for Testing and Materials (ASTM). ASTM E313. 2020. Standard practice for calculating yellowness and whiteness indices from instrumentally measured colour coordinates.
52. European Committee for Standardization (Comité Européen de Normalisation, CEN). EN 15802. 2009. Conservation of cultural property - Test methods - Determination of static contact angle.
53. European Committee for Standardization (Comité Européen de Normalisation, CEN). EN 14579. 2004. Natural stone test methods - Determination of sound speed propagation.
54. Guydader J, Denis A. 1986. Propagation des ondes dans les roches anisotropies sous contrainte évaluation de la qualité des schistes ardoisiers. *Bull. Eng. Geol. Environ.* 33:49-55. <https://doi.org/10.1007/BF02594705>
55. Fort R, Fernández-Revuelta B, Varas MJ, Álvarez de Buergo M, Taborda-Duarte M. 2008. Influence of anisotropy on the durability of Madrid-region Cretaceous dolostone exposed to salt crystallization processes. *Mater. Construcc.* 58(289-290):161-178. <https://doi.org/10.3989/mc.2008.v58.i289-290.74>
56. Fort R, Varas-Muriel MJ, Álvarez de Buergo Ballester M, Freire-Lista DM. 2011. Determination of anisotropy to enhance the durability of natural Stone. *J. Geophys. Eng.* 8(3):S132-S144. <https://doi.org/10.1088/1742-2132/8/3/S13>
57. American Society for Testing and Materials (ASTM). ASTM D4404. 2010. Standard test method for determination of pore volume and pore volume distribution of soil and rock by mercury intrusion porosimetry.
58. European Committee for Standardization (Comité Européen de Normalisation, CEN). EN 1936. 2006. Natural stone test methods - Determination of real density and apparent density, and of total and open porosity.
59. European Committee for Standardization (Comité Européen de Normalisation, CEN). EN 13755. 2008. Natural stone test methods - Determination of water absorption at atmospheric pressure.
60. Commissione di Normalizzazione Materiali Lapidei (NORMAL). Raccomandazione 7/81. 1981. Assorbimento d'acqua per immersione totale - Capacità di imbibizione.
61. European Committee for Standardization (Comité Européen de Normalisation, CEN). EN 15801. 2009. Conservation of cultural property - Test methods - Determination of water absorption by capillarity.
62. European Committee for Standardization (Comité Européen de Normalisation, CEN). EN 15803. 2009. Conservation of cultural property - Test methods - Determination of water vapour permeability (δp).
63. European Committee for Standardization (Comité Européen de Normalisation, CEN). International Organization for Standardization (ISO). EN ISO 16859-1. 2015. Metallic materials - Leeb hardness test - Part 1: Test method.
64. American Society for Testing and Materials (ASTM). ASTM D5873-14. 2023. Standard test method for determination of rock hardness by rebound hammer method.
65. Deere DU, Miller RP. 1966. Engineering classification and index properties for intact rock tech. Technical Report n° AFWL - TR-65-116. University of Illinois. <https://doi.org/10.21236/AD0646610>
66. Saptono S, Kramadibrata S, Sulistiano B. 2013. Using the schmidt hammer on rock mass characteristic in sedimentary rock at tutupan coal mine. *Procedia Earth Planet. Sci.* 6:390-395. <https://doi.org/10.1016/j.proeps.2013.01.051>
67. International Society for Rock Mechanics Commission. 1981. Rock characterization, testing and monitoring. ISRM suggested methods. Brown ET (ed.), Pergamon Press, Oxford.
68. Virella Torras A. 1964. Observación microscópica del clínker de cemento portland. *Mater. Construcc.* 14(113):23-30. <https://doi.org/10.3989/mc.1964.v14.i113.1791>
69. Elsen J. 2006. Microscopy of historic mortars - a review. *Cem. Concr. Res.* 36(8):1416-1424. <https://doi.org/10.1016/j.cemconres.2005.12.006>
70. Álvarez de Buergo Ballester M, González Limón T. 1994. Restauración de edificios monumentales. Estudio de materiales y técnicas instrumentales. Segunda edición. Monografía Centro de Estudios y Experimentación de Obras Públicas (CEDEX M-43).
71. Borrelli E, Laurenzi Tabasso M, Sánchez Martínez AE. 1996. Realización de muestras de mortero con cal aérea para el estudio de productos consolidantes: Propuesta metodológica. III Congreso Internacional de Rehabilitación del Patrimonio Arquitectónico y Edificación, 307-313, Granada, España.
72. Skoulikidis TH, Charalambous D, Tsakona K. 1996. Amelioration of the properties of hydrated lime for the consolidation of the surface or/and the mass of building materials of monuments or new buildings or statues and ornaments. In Proceedings of the 8th International Congress on Deterioration and Conservation of Stone, 1599-1605, Berlin, Germany.
73. Warr LN. 2021. IMA-CNMNC approved mineral symbols. *Mineral Mag.* 85(3):291-320. <https://doi.org/10.1180/mgm.2021.43>
74. Ergenç D, Gómez-Villalba LS, Fort R. 2018. Crystal development during carbonation of lime-based mortars in different environmental conditions. *Mater. Charact.* 142:276-288. <https://doi.org/10.1016/j.matchar.2018.05.043>
75. Steiner S, Lothenbach B, Proske T, Borgschulte A, Winnefeld F. 2020. Effect of relative humidity on the carbonation rate of portlandite, calcium silicate hydrates and ettringite. *Cem. Concr. Res.* 135:106116. <https://doi.org/10.1016/j.cemconres.2020.106116>

76. Allen G, Allen J, Elton N, Farey N, Holmes S, Livesey P, Radonjic M. 2003. Hydraulic lime mortar for stone. Brick and block masonry. Donhead Publishing Ltd. Dorset.
77. Kozlovcev P, Prikryl R. 2015. Devonian micritic limestones used in the historic production of Prague hydraulic lime ('pasta di Praga'): characterization of the raw material and experimental laboratory burning. *Mater. Construcc.* 65(319):e060. <https://doi.org/10.3989/mc.2015.06314>
78. Válek J, Van Halem E, Viani A, Pérez-Estébanez M, Sevcík R, Sasek P. 2014. Determination of optimal burning temperature ranges for production of natural hydraulic limes. *Constr. Build. Mater.* 66:771-780. <https://doi.org/10.1016/j.conbuildmat.2014.06.015>
79. Kozlovcev P, Válek J. 2021. The micro-structural character of limestone and its influence on the formation of phases in calcined products: natural hydraulic limes and cements. *Mater. Struct.* 54:217. <https://doi.org/10.1617/s11527-021-01814-7>
80. Gualtieri AF, Viani A, Montanari C. 2006. Quantitative phase analysis of hydraulic limes using the Rietveld method. *Cem. Concr. Res.* 36(2):401-406. <https://doi.org/10.1016/j.cemconres.2005.02.001>
81. Artioli G, Secco M, Addis A. 2019. The Vitruvian legacy: Mortars and binders before and after the Roman world. Artioli G, Oberti R (eds.). *The contribution of mineralogy to cultural heritage.* 151-202. <https://doi.org/10.1180/EMU-notes.20.4>
82. Collepari M. 2003. A state-of-the-art review on delayed ettringite attack on concrete. *Cem. Concr. Compos.* 25(4-5):401-407. [https://doi.org/10.1016/S0958-9465\(02\)00080-X](https://doi.org/10.1016/S0958-9465(02)00080-X)
83. Palomo A, Blanco-Varela MT, Martínez-Ramírez S, Puertas F, Fortes C. 2002. Historic mortars: characterization and durability. new tendencies for research. Advanced Research Centre for Cultural Heritage: Interdisciplinary Projects. In Fifth Framework Programme Workshop, Brussels, Belgium.
84. Farcas F, Touzé P. 2001. La spectrométrie infrarouge à transformée de Fourier (IRTF). Une méthode intéressante pour la caractérisation des ciments. *Bull. Lab. Ponts Chaussées.* 230(4350):77-88.
85. Diekamp A, Stalder R, Konzett J, Mirwald PW. 2012. Lime mortar with natural hydraulic components: Characterisation of reaction rims with FTIR imaging in ATR-mode. Válek J, Hughes JJ, Groot CJWP (eds). In *Historic Mortars: Characterisation, assessment and repair*, RILEM Bookseries, vol 7. Springer, Dordrecht, 105-113. https://doi.org/10.1007/978-94-007-4635-0_8
86. Földvári M. 2011. Handbook of thermogravimetric system of minerals and its use in geological practice, Geological Institute of Hungary, Budapest.
87. Fort R, Varas-Muriel MJ, Ergenç D, Cassar J, Anastasi M, Vella NC. 2023. The technology of ancient lime mortars from the Zejtun Roman Villa (Malta). *Archaeol. Anthropol. Sci.* 15:15. <https://doi.org/10.1007/s12520-022-01710-3>